ANALYSIS OF THERMAL EVOLUTION IN TEXTILE FABRICS USING ADVANCED MICROSTRUCTURE SIMULATION TECHNIQUES

MATTHIAS RÖMMELT[*], ANASTASIA AUGUST[2], BRITTA NESTLER[2] AND ARON KNEER[1]

[*],[1] TinniT Technologies GmbH
Erbprinzenstr. 32, 76133 Karlsruhe, Germany
Email: info@tinnit.de - Web page: http://www.tinnit.de/

[2] Karlsruhe Institute of Technology
Institute for Applied Matererials
Haid-und-Neu-Str. 7, 76131 Karlsruhe, Germany
Email: anastasia.august2@kit.edu - Web page: http://www.iam.kit.edu/zbs

Key words: CFD, Environmental Technologies, Numerical Methods, Textile Composites, Thermal Evolution

Abstract. Nowadays, membrane structures represent a modern construction element to be used as roof material in modern buildings or as design element in combination with traditional architecture. Membranes are mostly used in an outdoor environment. Therefore they are exposed to wind, radiation (solar and infrared), rain and snow. Specific membranes are three-dimensional fabrics which can be used as energy absorber or as insulation of membrane roofs. The applicability as energy absorber becomes important if the three-dimensional fabrics are designed as a porous flow channel streamed by air and convectively heated up. The transferred energy may be stored in a latent heat storage system.

Due to their porous structure, textile fabrics have a large heat-exchanging surface. If they are handled as homogenized porous structures, the heat transfer processes can not be described in a correct way. Therefore a microstructure model locally resolving all filaments of the three-dimensional fabrics has been formulated. By using an advanced meshing tool, a simulation technique has been developed taking into account the local heat conduction properties of the different materials.

To analyse the heat transfer processes inside the three-dimensional fabrics, numerical simulations have been performed using the phase-field solver (Pace3D) of the Karlsruhe Institute of Technology and the commercial CFD-Solver StarCCM+. For a better understanding of the thermal behaviour of the fabrics, different thermal loads including thermal conduction in the microstructure (filaments) and convection by the surrounding air have

been computed. The results show that the advanced simulation techniques allow to analyse the rate of conductive and convective heat transfer in three-dimensional fabrics. The results of the applied computational methods are compared.

1   INTRODUCTION

As a part of the polar bear project, a textile pilot building is constructed. The textile structure is used to generate heat and copy the fur of the polar bear [3]. The use of textile structures as a thermal collector offers many advantages. Textile structures are flexible and can be used as a self-supporting roof or on rooftops. Here, in addition to generating heat, the insulation is important. In the future textile structures will be used on roofs with an area ranging from several up to 10000 m^2.
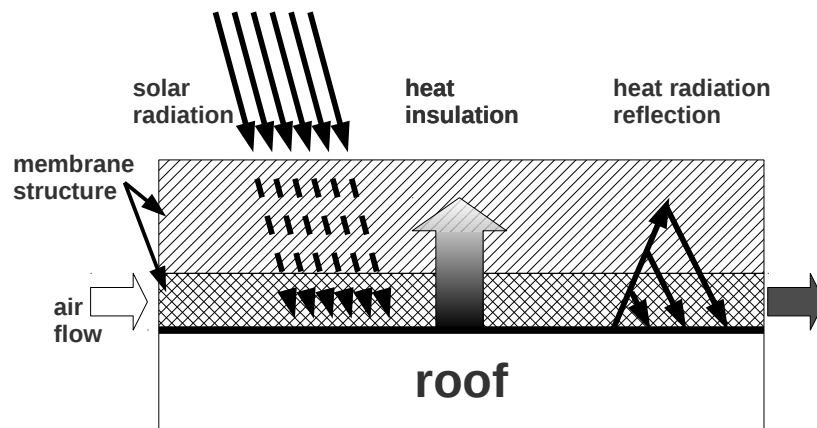

Figure 1: Design and principle of a thermal collector with membrane structures.

The operating principle is shown in Figure 1. To have a well insulating textile fabric that can be used as a thermal heat collector, it must have the following characteristics:

1. Solar radiation should be transmitted.

2. Heat radiation from the roof and the heated structure should be reflected.

3. The textile fabric should have a low thermal conductivity.

4. Flowing through air should absorb heat from the textile fabric.

The solution is a construction of three different textile structures. Figure 2 shows the structure. Layer 2 and 3 transmit solar radiation and reflect heat radiation. Layer 1
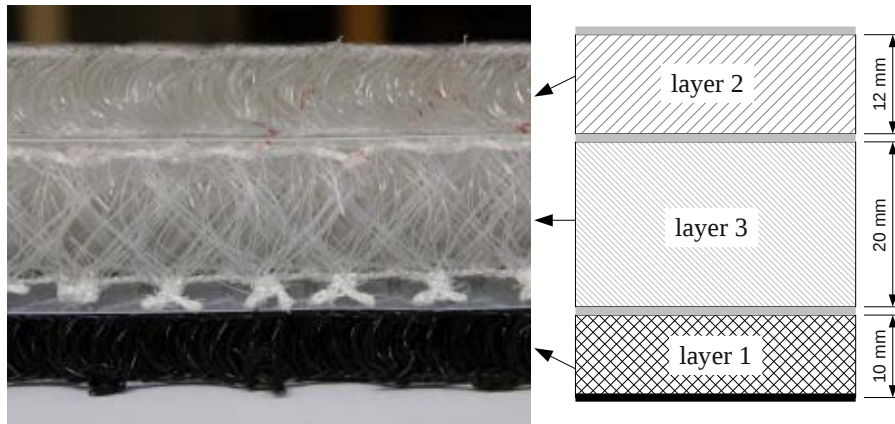
Figure 2: Thermal collector composed of 3 layers of textile spacer fabrics.

absorbs solar radiation and air flows through. All three layers act as insulation. In the following property 3 and 4 are considered in more detail.

To calculate the physical processes in the textile, a detailed model resolving the structure is needed. The complete structure is required for the calculation of heat conduction, the surface for convective heat transfer. The textile membranes are used industrially on a large scale. It is not possible to calculate large areas of textile structures with resolution of the finest fibers with today's computing capacity. Therefore, it is necessary to reproduce small units of the textile structure with all the fibres in a representative volume. Using these models the physical processes are calculated and we obtain, for example, a temperature profile or a pressure profile within the structure. Thus it is possible to better understand the processes in the textile structure and to calculate effective material parameters and dimensional parameters for the modeled structure unit. Effective material parameters and dimensionless parameters allow a calculation of large areas, because instead of an exact resolution of the structure, effective material parameters are used.

The following sections explain the pre-processing, calculation, evaluation and determination of effective material parameters for the textile structure in Figure 2.

2 PREPROCESSING

The model generation is described for layer 1 in Figure 3. In a first step, the structure is analysed. The structure consists of three different textile fiber elements, which recur periodically within the tissue. The geometric dimensions of the structure and the individual structural elements are required for the reconstruction.

In a second step the individual structural elements are replicated. Therefore the program Pace3D was used. Pace3D stands for Parallel Algorithm in Crystal evolution in 3D. The software package was developed for materials science applications in order to

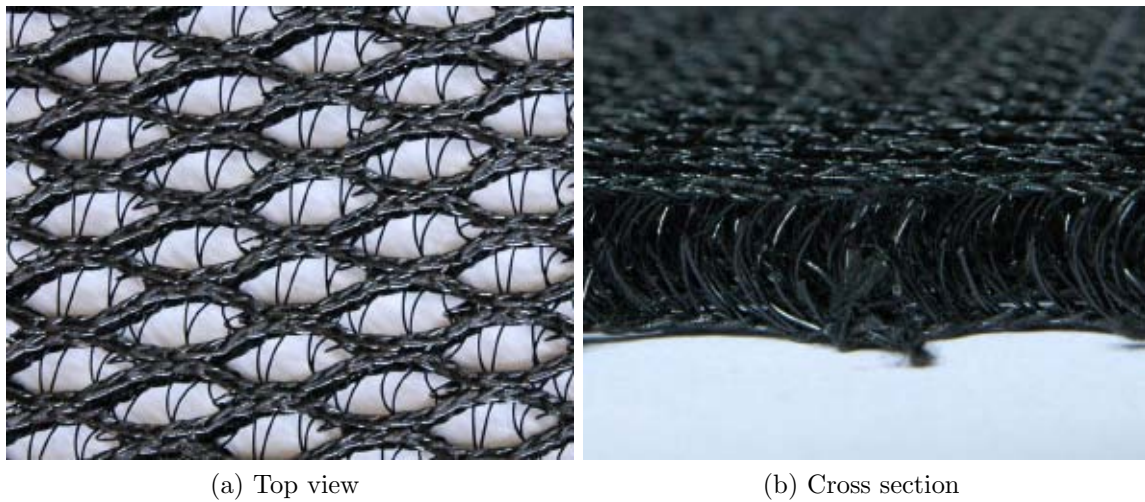(a) Top view   (b) Cross section

Figure 3: Textile spacer fabrics at high resolution.

computationally design new materials with tailored properties and to get insight in microstructure formation processes. The mathematical and physical basis is a phase-field model [2]. Within the simulation program, a volume is defined which is discretized with hexahedrons. Each hexahedron is assigned a phase, the structure gets a solid phase and the surrounding air a gaseous phase. To model the structure area, the preprocessing of

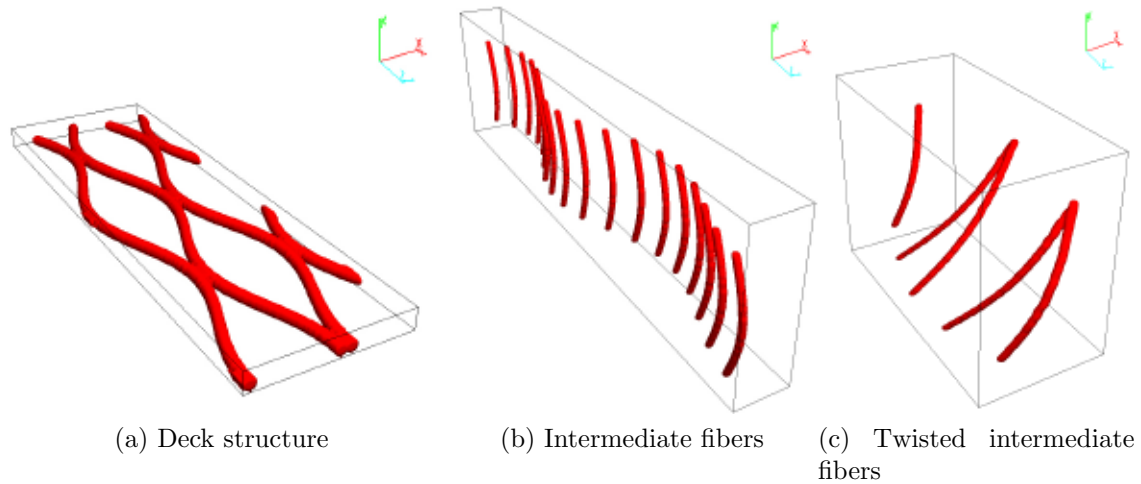(a) Deck structure   (b) Intermediate fibers   (c) Twisted intermediate fibers

Figure 4: Design elements to construct layer 1.

the software provides interfaces to define functional expressions to describe the three-

dimensional geometry. In the case of the deck fibre, it is a sine function

$$F1(z) = amp \cdot \sin\left(z \cdot \frac{2\pi}{\lambda}\right) \ . \tag{1}$$

The parameters were taken from the geometric dimensions. The fiber was then multiplied to get the deck structure.

When creating the second structure type, the intermediate fibers, the procedure was comparable. They were also modeled with a sine function. The duplication of the fiber is based on the sine function in equation (1). The twisted intermediate fibers form the third type of fiber. They have the special feature keeping overlying deck fibres seperate and connecting diagonally above the other deck fiber. Therefore, two functions overlap, a linear shift in x-direction and a sine-function in z-direction. Figure 4 shows the three structural elements.

In a third step, the structural elements are combined and superimposed. The result is the overall structure in Figure 5a. Layer 2 and 3 were created similarly. They are shown

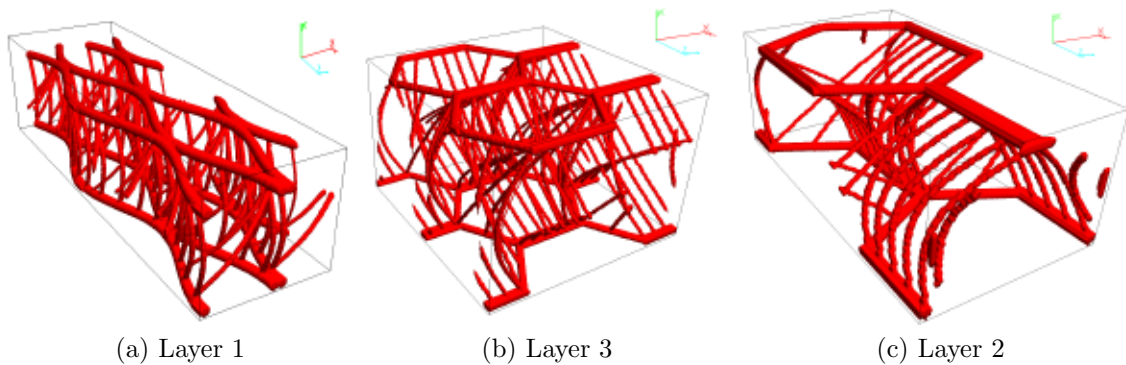| (a) Layer 1 | (b) Layer 3 | (c) Layer 2 |

Figure 5: Modeled layers of the thermal collector.

in Figure 5b and 5c.

By formulating suitable mathematical expressions, a twisted deck fiber in Figure 6 can be generated. It is composed of four single fibers twisted together and shaped in the form of a sine curve. In the further refinement of the structure it has to be estimated, whether this improves the accuracy of the calculation or just increases the computational cost and complexity.

3 CALCULATED LOADCASES

Based on the structural model in Figure 5a different calculations were performed. In addition to Pace3D, StarCCM+ was used for calculation. StarCCM+ is a commercial Computational Fluid Dynamics (CFD) code. There were three aims:

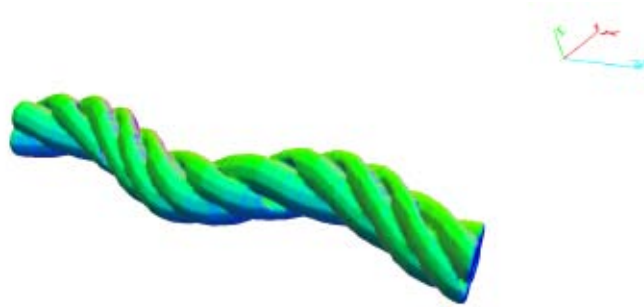- Analysis of physical processes in the structures

Figure 6: Twisted deck structure fiber.

- Comparing the results of Pace3D and StarCCM+

- Calculation of effective material parameters

For this purpose two load cases LC1 and LC2 were defined. The textile fabric is made of polyamide surrounded by air. The used material parameters are given in Table 1 and are taken from the VDI-Wärmeatlas [1].

Material	Polyamide	Air
	$T = 323.15\ K$	$T = 333.15\ K$
Density $\rho\ \left[\frac{kg}{m^3}\right]$	$1150.0_{(T=293.15\ K)}$	1.046
Heat capacity $c_p\ \left[\frac{J}{kg \cdot K}\right]$	1680.0	1008.2
Heat conductivity $\lambda\ \left[\frac{W}{m \cdot K}\right]$	$330.0 \cdot 10^{-3}$	$28.8 \cdot 10^{-3}$
Dynamic viscosity $\nu\ \left[\frac{m^2}{s}\right]$	-	$192.2 \cdot 10^{-7}$

Table 1: Material values for LC1 und LC2.

3.1 Load case LC1

We calculated the steady-state heat conduction through the textile structure. For the calculation, the smallest periodic unit (unit cell) of the textile structure was considered and model-appropriate temperature conditions imposed. Figure 7a shows the selected boundary conditions. For the calculation with Pace3D, also a base plate was added (Figure 7c). The base plate is made of polyamide and has the height $\Delta y = 1\ mm$. Using this base plate it is possible to calculate the heat flow through the structure. For the calculation with StarCCM+ the construction of a base plate is not necessary (Figure 7b).

Due to the non-stationary solution scheme of Pace3D, the simulation has to run for a long physical time until a steady-state temperature profile has formed over the structure.
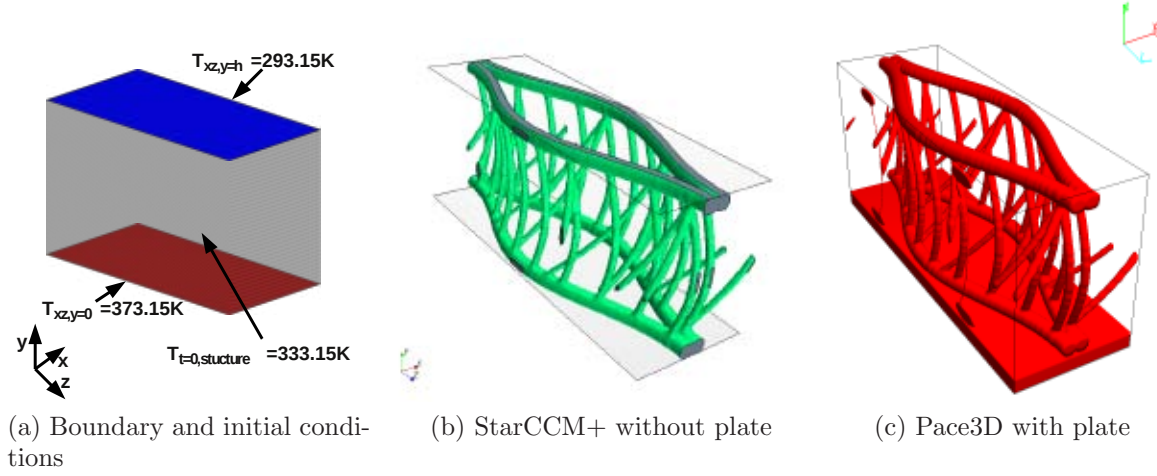
(a) Boundary and initial conditions

(b) StarCCM+ without plate

(c) Pace3D with plate

Figure 7: Boundary conditions and simulation environment (LC1).

This is reached after about $100\ s$. In addition, the initial conditions were chosen so, that they are close to a steady-state temperature profile. For the textile structure, we chose $T_{t=0,structure} = 333.15\ K$ and for the base plate $T_{t=0,plate} = 373.15\ K$. StarCCM+ calculates at steady-state conditions and implicitly, therefore the required computing time is lower.

3.2   Load case LC2

For load case LC 2, four unit cells like in Figure 7b were joined together. This structural unit is flown through by air in a channel and heated from below with a temperature $T_{yz,x=0} = 373.15\ K$. The structure and air are heated. The convective and conductive heat transfer and pressure loss are considered. Figure 8 shows the geometry and boundary conditions. The channel has a length of $L_{channel} = 210\ mm$. The structure is passed through in the direction of the x-axis with a speed of $u = 1.0\ \frac{m}{s}$. The temperature of the fluid at the inlet is $T_{inlet} = 293.15\ K$. To estimate the Reynolds number, a channel cross-section between two intermediate fibers of $d = 1.75\ mm$ and an increased flow velocity of $u_{max} = 2.0\ \frac{m}{s}$ is assumed. It results in a Reynolds number of

$$Re = \frac{u_{max} \cdot d}{\nu} = 182.1\ .\qquad(2)$$

The flow has established steady-state and remains at laminar conditions.

4   RESULTS

The LC1 for the layer 1 was calculated with Pace3D and StarCCM+. The results illustrate the temperature layers in Figure 9a for stationary state. Figure 9b shows the
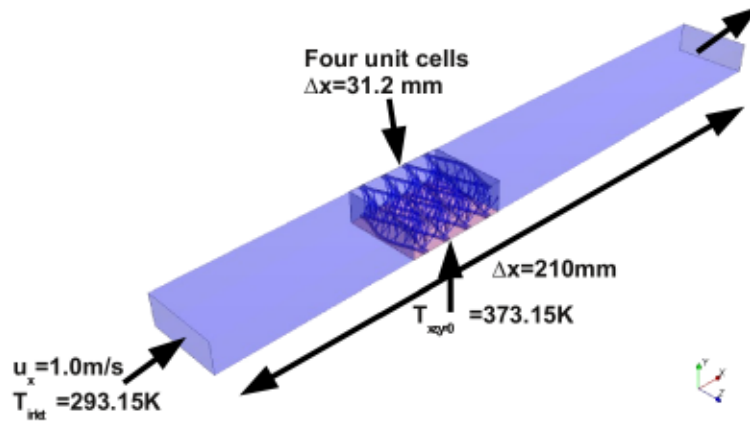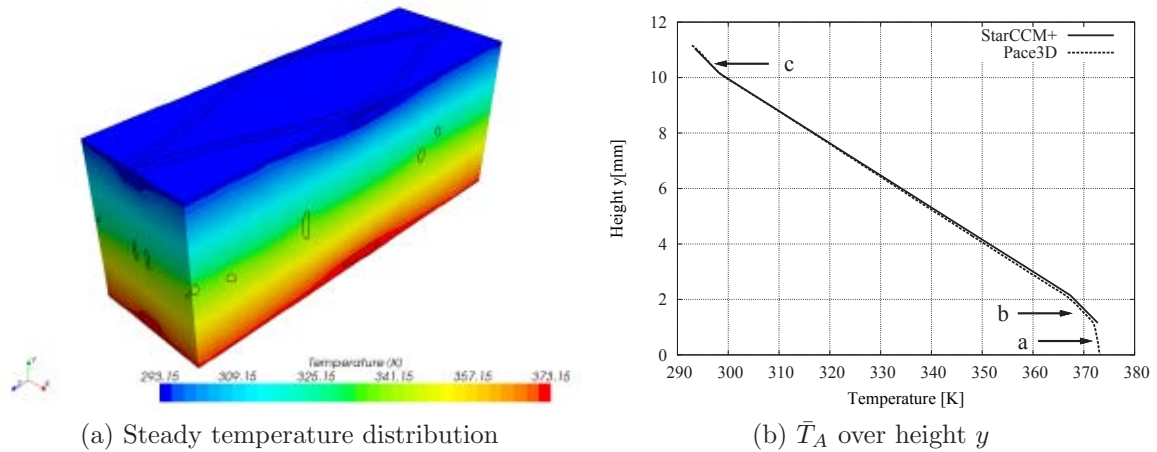
Figure 8: Geometry and boundary conditions (LC2).

(a) Steady temperature distribution

(b) $\bar{T}_A$ over height y

Figure 9: Temperature distribution and profile.

temperature distribution over the height of the structure. The diagram was obtained by averaging the temperature over the xz-plane.

The heat flow through the structure is calculated with StarCCM+ as $\dot{Q} = 60.2 \cdot 10^{-3}\ W$. For Pace3D, the heat flow can be calculated using the temperature difference over the base plate. The temperature difference is $\Delta T = 0.9\ K$. With the corresponding geometric values, we get $\dot{Q} = 56.2 \cdot 10^{-3}\ W$ using

$$\dot{Q} = \frac{\lambda}{\Delta y} \cdot \Delta T \cdot A \ . \tag{3}$$

LC2 was calculated for layer 1 with StarCCM+. Figure 10 shows the stationary temperature profile for the xy-plane. By the hot plate, heat is applied to the structure and the

Variable	StarCCM+	Pace3D
Area $A = \Delta x \cdot \Delta z \ [m^2]$	$185.2 \cdot 10^{-6}$	$189.3 \cdot 10^{-6}$
Height $\Delta y_{structure} \ [m]$	$9.9 \cdot 10^{-3}$	$10.2 \cdot 10^{-3}$
Temperature difference $\Delta T_{structure} \ [K]$	80	79.4
Heat flow $\dot{Q} \ [W]$	$60.2 \cdot 10^{-3}$	$56.2 \cdot 10^{-3}$

Table 2: Geometric values and results of LC1.
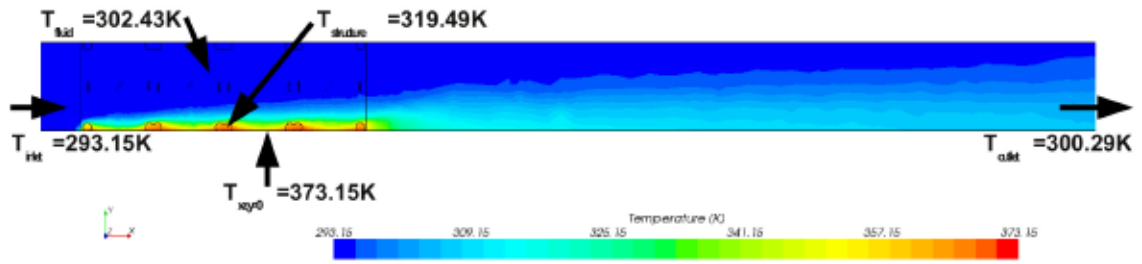
Figure 10: Temperature distribution in the xy-layer (LC2).

air. The air is heated from $T_{inlet} = 293.15 \ K$ to $T_{outlet} = 300.29 \ K$. The supplied heat energy is $\dot{Q} = 1.762 \ W$. The averaged temperature of the structure is $\bar{T}_{structure} = 319.49 \ K$ and of the air between the structure $\bar{T}_{fluid} = 302.43 \ K$.
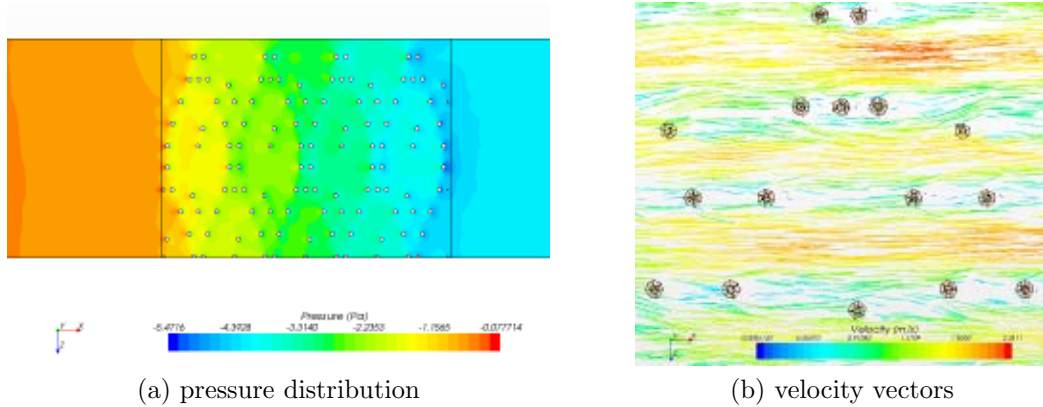
(a) pressure distribution

(b) velocity vectors

Figure 11: Pressure distribution and velocity vectors for the xz-layer (LC2).

During flow through the structure, a stagnation point is formed in front of the fibers. Between the fibers, the flow is accelerated due to the cross-section. Figure 11a depicts

the pressure distribution over the structure. The pressure loss during flow through the structure is $\Delta p = 3.7\ Pa$. Figure 11b displays the velocity vectors in the xz-plane for a part of the structure. The velocity vectors reveal the flow around the individual fibers. To reflect these phenomena within the structure, it is necessary to accurately reproduce the structure. The maximum speed discovered in the computational domain is $u_{max} = 2.28\ \frac{m}{s}$. With this value, our estimation used to calculate the Reynolds number turns out to be correct.

5 DISCUSSION

The results of the temperature versus height y in Figure 9b and obtained by StarCCM+ and Pace3D are almost identical. Position a) in the diagram shows the temperature curve above the base plate. Position b) and c) correspond to the lower and upper deck structure. Here the proportion of polyamide is higher than in the area of the intermediate fibers. The thermal conductivity is greater in these areas, because they have a lower temperature gradient. The proportion of polyamide and the course of the fibers have an influence on the thermal conductivity. For technical applications, the effective thermal conductivity of the entire structure is important. This is given by

$$\lambda_{eff} = \frac{\dot{Q} \cdot \Delta y_{structure}}{\Delta T_{structure} \cdot A} \ . \tag{4}$$

With the values from Table 2 for the layer 1, the effective thermal conductivities of the two simulation applications are $\lambda_{eff,StarCCM+} = 40.2 \cdot 10^{-3}\ \frac{W}{K \cdot m}$ and $\lambda_{eff,Pace3D} = 38.1 \cdot 10^{-3}\ \frac{W}{K \cdot m}$. The deviation of the calculated values is 5.2% with respect to $\lambda_{eff,StarCCM+}$. This small difference and the similar temperature distribution in Figure 9b serve as a validation of the results. LC1 was also used for the layers 2 and 3 with StarCCM+, and

Layer	$\lambda_{eff}\ [\frac{W}{m \cdot K}]$	$c_p\ [\frac{J}{kg \cdot K}]$	$\rho\ [\frac{kg}{m^3}]$
Layer 1	$40.2 \cdot 10^{-3}$	1048.5	70.0
Layer 2	$33.4 \cdot 10^{-3}$	1026.5	32.4
Layer 3	$32.8 \cdot 10^{-3}$	1018.7	19.1
Complete structure	$34.4 \cdot 10^{-3}$	1027.8	34.6

Table 3: Calculated values for the three layers with StarCCM+ (LC1).

the effective thermal conductivity was calculated. Table 3 contains the resulting values. With the effective thermal conductivity of the three layers, it is possible to determine an effective thermal conductivity for the whole structure of $\lambda_{eff,tot} = 34.4 \cdot 10^{-3}\ \frac{W}{m \cdot K}$, which is 19.4% larger than the thermal conductivity of pure air. The whole structure has good thermal insulating properties similar to air. This value can be used for technical design

of large textile surfaces. In conclusion, the thermal insulation properties can be correctly reproduced without resolution of the exact structures.

Another important feature to evaluate and interpret is the heat transfer from the structure to the fluid. The heat transfer coefficient α specifies the transferred heat power per surface and temperature difference. For textile membranes, there is no valid Nusselt number correlation. With the values of the LC2, the heat transfer coefficient for layer 1 can be estimated to

$$\bar{\alpha} = \frac{\dot{Q}}{A_{structure} \cdot (T_{structure} - T_{fluid})} \ , \tag{5}$$

where $A_{structure} = 2.26 \cdot 10^{-3} \ m^2$ is the interface area between fluid and structure. This results in an averaged value of $\bar{\alpha} = 139.1 \ \frac{W}{m^2 \cdot K}$. For comparison, the heat transfer coefficient for an overflown, heated plate was calculated to $\bar{\alpha} = 22.0 \ \frac{W}{m^2 \cdot K}$ by the correspondig Nusselt number correlation of the VDI-Wärmeatlas [1]. The heat transfer in the flow is increased by the structure. The heat is taken away from the structure by the air flowing through, and can be stored for example in a latent heat storage.
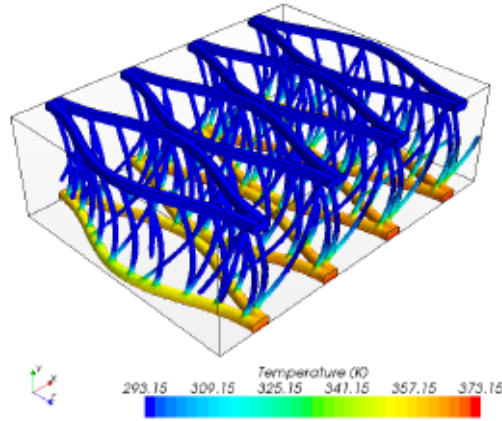

Figure 12: Temperature distribution in the textile fiber.

As seen in Figure 10, the heat only penetrates into the flow region at the bottom of the channel. Figure 12 emphasizes this, the fiber is heated only in the lower third. The corresponding Biot number is the heat transfer between fluid and structure in relation to heat conduction in the structure. It can be estimated with $\bar{\alpha}$ as

$$Bi = \frac{\bar{\alpha} \cdot L_{structure}}{\lambda_{structure}} \ . \tag{6}$$

The characteristic length of the structure $L_{structure}$ is given by the structure height $\Delta y = 9.85 \cdot 10^{-3} \ m$ and $\lambda_{structure} = 330.0 \cdot 10^{-3} \ \frac{W}{m \cdot K}$ refers to $\lambda_{Polyamide}$. This results in the
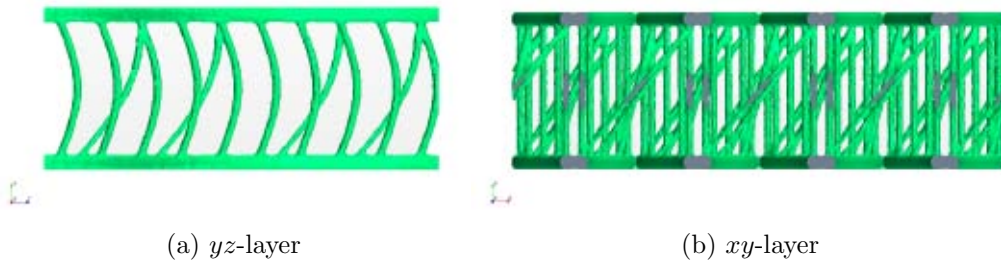
(a) yz-layer

(b) xy-layer

Figure 13: Cross-sections of the structure.

dimensionless number $Bi = 4.2$. A Biot number greater one means that the heat transfer in the flow is greater than the heat conduction in the structure. Therefore the structure is heated marginal. The heat is completely removed at the bottom of the structure by the fluid. In technical applications, the structure is heated by radiation leading to a more uniform heat distribution and to higher heat transfer rates.

The flow through the structure yields not only an improved heat transfer, but also results in increased pressure loss important for applications to fans. To make advantage of this property, the structure was designed, so that, in the direction of flow, channels are formed (Figure 13a). The flow resistance is reduced. The view in Figure 13b shows an almost closed fiber structure for which the resistance for a flow in z-direction increases.

6   CONCLUSION

The microstructure simulation software Pace3D is capable to recreate small units of textile structures. All fibers and surfaces relevant to reflect physical processes have been modelled. With defined load cases, these processes were examined in the textile structures. The stationary heat conduction in three textile structures was simulated with StarCCM+ and Pace3D and an effective thermal conductivity was calculated. It was shown that the textile structures have good thermal insulation properties.

In a second load case, the flow through a textile structure was simulated with Star-CCM+. The convective and conductive heat transfer and pressure loss were calculated. The textile structure develops a higher heat transfer coefficients α. The Biot number and analysis of the temperature distribution in the structure indicate that the heat conduction in the structure is an insufficient heat transfer mechanism. This is because of the low thermal conductivity of the polyamide and the large surface of the structure.

A comparative analysis of stationary heat conduction with Pace3D and StarCCM+ showed almost identical results and served as validation of the two different approaches. Based on the results, predictions can be made about the influence of the particular structure of textile fabrics on heat transfer properties. Effective material parameters can be calculated for the structures starting from this detailed analysis.

For the complete design of thermal collectors, made of textile membranes, a forthcoming research will adress the following issues:

- the definition of additional load cases

  - to study the radiation behaviour of textile structures.
  - to create a pressure correlation for calculating the pressure drop at different operating points and flow lengths.

- validation by experimental data.

- structural optimization considering the required heat and flow characteristics.

REFERENCES

[1] *VDI-Wärmeatlas.* VDI Buch. Springer, Berlin, 10. edition, 2006. 3, 5

[2] B. Nestler, H. Garcke, and B. Stinner. Multicomponent alloy solidification phasefield modelling and simulations. *Physical Review*, 71, 2005. 2

[3] T Stegmaier, M. Linke, and H Planck. Bionics in textiles: flexible and translucent thermal insulations for solar thermal applications. *Phil. Trans. R. Soc.*, (367):1749–1758, 2009. 1